

Serrated Flow Behavior of Aisi 316L Austenitic Stainless Steel for Nuclear Reactors

Qingshan Li¹, Yinzong Shen^{1,*} and Pengcheng Han¹

¹School of Mechanical Engineering, Shanghai Jiao Tong University, No.800 Dongchuan Road, Shanghai 200240, China
Email: shenyz@sjtu.edu.cn

Abstract. AISI 316L austenitic stainless steel is a candidate material for Generation IV reactors. In order to investigate the influence of temperature on serrated flow behavior, tensile tests were performed at temperatures ranging from 300 to 700 °C at an initial strain rate of $2 \times 10^{-4} \text{ s}^{-1}$. Another group of tensile tests were carried out at strain rates ranging from 1×10^{-4} to $1 \times 10^{-2} \text{ s}^{-1}$ at 600 °C to examine the influence of strain rates on serrated flow behavior. The steel exhibited serrated flow, suggesting the occurrence of dynamic strain ageing at 450-650°C. No plateau of yield stresses of the steel was observed at an initial strain rate of $2 \times 10^{-4} \text{ s}^{-1}$. The effective activation energy for serrated flow occurrence was calculated to be about 254.72 kJ/mol⁻¹. Cr, Mn, Ni and Mo solute atoms are expected to be responsible for dynamic strain ageing at high temperatures of 450-650 °C in the steel.

1. Introduction

AISI 316L austenitic stainless steel has been extensively applied in reactor vessel and piping systems. This steel is a candidate material for Generation IV nuclear reactors due to its excellent corrosion resistance, tensile and creep strength at elevated temperature, and enhanced resistance to sensitization and intergranular cracking [1]. Serrated flow, negative strain rate sensitivity, ductility minima and peak/plateau in yield strength are often observed in the austenitic stainless steels, such as types 304L and 316L stainless steels, which are characteristics of dynamic strain ageing (DSA). The phenomenon of DSA is also known as Portevin Le-Chatelier (PLC) effect, which is significant to austenitic stainless steels for the service temperature and DSA temperature regime overlap [2]. The occurrence of DSA has significant influence on mechanical properties, for example, increasing strength and decreasing ductility [3]. As a consequence, it is of great significance to research the characteristics and mechanism of DSA of AISI 316L austenitic stainless steel at elevated temperatures.

The test parameters such as applied strain rate, temperature and several material variables have a great influence on the behavior of serrated flow. In this paper, we focus on the serrated flow behavior of AISI 316L austenitic stainless steel through tensile tests at temperatures of 300-700 °C at a strain rate of $2 \times 10^{-4} \text{ s}^{-1}$ and at various strain rates at 600°C. Additionally, the mechanism of serrated flow in AISI 316L austenitic stainless steel at elevated temperatures is discussed.

2. Experiment Procedures

The steel employed in this study is commercial AISI 316L austenitic stainless steel. The steel was solution treated at 1100 °C for 40 min, then cooled in water to room temperature. The composition (in wt pct) of the steel is 0.033 C, 0.8937 Mn, 0.271 Si, 16.56 Cr, 9.985 Ni, 2.094 Mo, 0.028 P, 0.0088 S. Specimens originated from a forged bar with a diameter of 18 mm. Tensile specimens with a gauge



diameter of 10 mm and a gauge length of 25 mm were machined by wire-electrode cutting. Before tensile test, specimens were carefully polished using metallographic sandpaper.

Tensile tests were carried out on Shimadzu AG-100KNA machine within $\pm 0.3\%$ of indicated test force. For elevated temperature tests, temperature can be controlled within $\pm 10^\circ\text{C}$. Data was recorded using a data acquisition system attached to the tensile test system. Tensile tests were carried out at temperatures ranging from 300 to 700 $^\circ\text{C}$ at an initial strain rate of $2 \times 10^{-4} \text{ s}^{-1}$ to investigate the influence of temperature on mechanical properties of the steel. Another group of tensile test was performed at strain rates ranging from 1×10^{-4} to $1 \times 10^{-2} \text{ s}^{-1}$ at 600 $^\circ\text{C}$ to examine the influence of strain rate on serrated flow behavior of the steel.

3. Results and Discussion

The figure 1(a) illustrates the variation of yielding and ultimate tensile strengths with temperature at a strain rate of $2 \times 10^{-4} \text{ s}^{-1}$. Normally, ultimate tensile strength drops significantly as temperature rise in elevated temperature tensile test. However, ultimate tensile strength decreases slightly, while yielding strength changes inconspicuously at intermediate temperatures of 450-650 $^\circ\text{C}$. Figure 1(b) shows the variation of elongation with temperature. With increasing tensile temperature, elongation first increases slightly, and then decrease occurred at 400-500 $^\circ\text{C}$ and 500-600 $^\circ\text{C}$. DSA is the phenomenon that strain and ageing occur simultaneously during deformation process. Since ageing has significant influence on strength and ductility, not only increase in ultimate and yielding strengths but also decrease in elongation are attributed to the occurrence of DSA, which can be explained by the mechanism of ageing strengthening. With the increase of interactions of solute atoms with dislocations during DSA, the dislocation density is enhanced so that ductility is decreased [4].

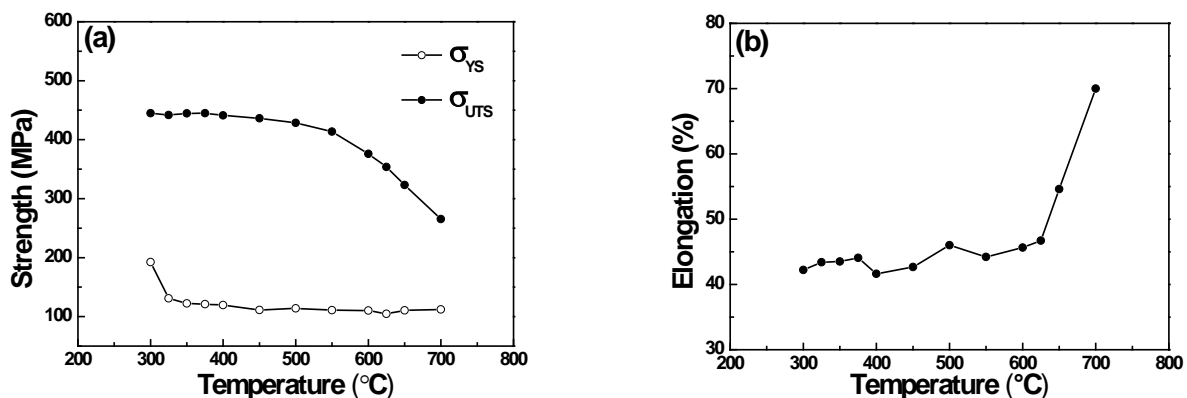


Figure 1. The variation of tensile properties with temperature at an initial strain rate of $2 \times 10^{-4} \text{ s}^{-1}$ (a) ultimate tensile strength and yielding strength, (b) elongation.

In general, stress-strain curves are smooth during tensile plastic deformation, in the case of present tensile tests, stress-strain curves remain smooth at low temperatures below 400 $^\circ\text{C}$, while serrations occurred on stress-strain curve when tensile temperature reached 450 $^\circ\text{C}$. Figure 2 shows segments of tensile curves at various temperatures at a strain rate of $2 \times 10^{-4} \text{ s}^{-1}$. Serrated flow can be observed at intermediate temperatures of 450-650 $^\circ\text{C}$. However, serrated flow disappeared at 700 $^\circ\text{C}$ and tensile curve became smooth again. Other researchers studied the DSA of AISI 316L austenitic stainless steel. Kim [5] found serrations in the temperature of 400-600 $^\circ\text{C}$ at a strain rate of $2 \times 10^{-4} \text{ s}^{-1}$. Samuel's [6] research suggested that serrations were observed in the temperature of 450-650 $^\circ\text{C}$ at a strain rate of $3 \times 10^{-4} \text{ s}^{-1}$. Choudhary's [2] tests were carried out at a strain rate of $3.16 \times 10^{-4} \text{ s}^{-1}$. They found that serrations were first found at 300 $^\circ\text{C}$, mild serrations appeared at 327 $^\circ\text{C}$, stress-strain curves were smooth at 350 $^\circ\text{C}$ -375 $^\circ\text{C}$, mild serrations appeared again at 400-425 $^\circ\text{C}$ and serrations reappeared in the temperature range of 450-650 $^\circ\text{C}$.

Different types of serrations appearing on the stress-strain curves at various temperatures have been classified into types A, B and C serrations. Type A serrations exhibit an abrupt rise in the loads followed by discontinuous drops to or below the general level of tensile curves due to periodic locking

of dislocations. They usually occur in the condition of low temperature or high strain rate. The type B serrations are discontinuous and fine scale oscillations about the general level of the stress-strain curve and Type B serrations often develop following the occurrence of type A serrations. Type C serrations

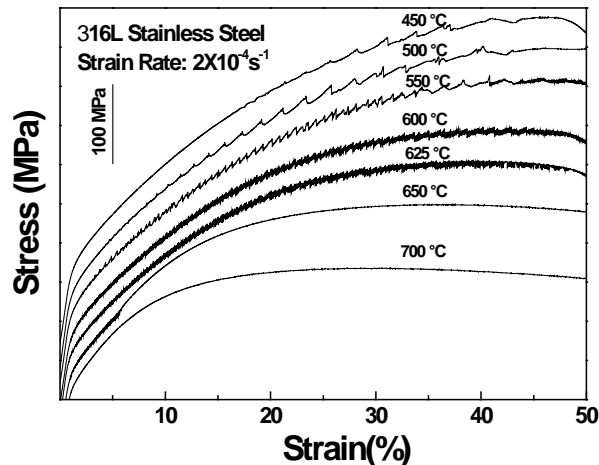


Figure 2. Tensile curves at various temperatures at an initial strain rate of $2 \times 10^{-4} \text{ s}^{-1}$

are always below the general level of stress-strain curve. The segments of various types of serrations at different temperatures are showed in figure 3(a) and figure 3(b) Type A serrations appeared at 450 °C and 500 °C, and mixed type A+B serrations appeared at 550-625 °C. However, mixed type A+B serrations converted to Type C serrations at 625 °C. At 650 °C, type C serrations occurred during the early stage of tensile deformation, and serrations disappeared as deformation proceeds. In Choudhary's test, type C serrations were observed to intersperse between type A serrations at 650 °C [2].

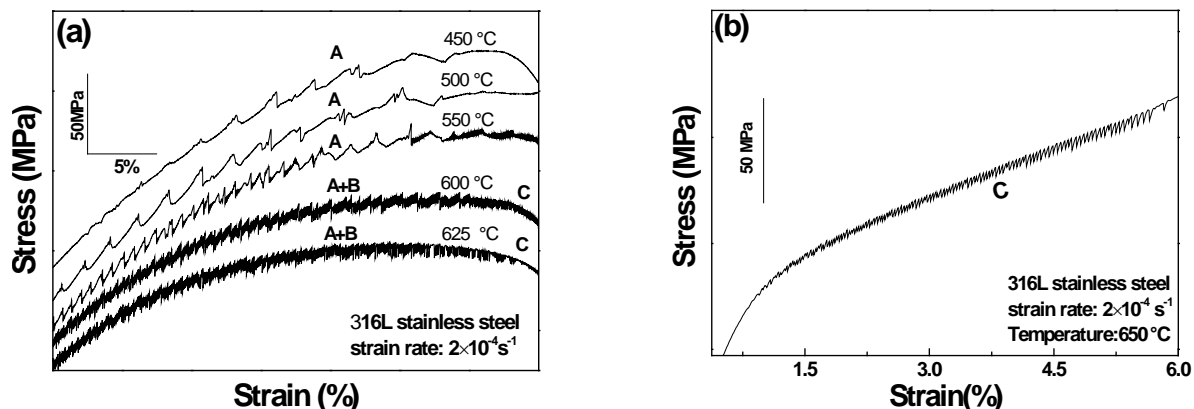


Figure 3. Segment of tensile curves (a) at various temperatures at an initial strain rate $2 \times 10^{-4} \text{ s}^{-1}$ and (b) at 650 °C at an initial strain rate of $2 \times 10^{-4} \text{ s}^{-1}$

The segment of stress-strain curves are shown in figure 4. It was found that mixed type A+B serrations appeared at 600 °C at strain rates of 1×10^{-4} and $2 \times 10^{-4} \text{ s}^{-1}$, while type A serrations appeared at strain rates of 2×10^{-3} , 6×10^{-3} and 10^{-2} s^{-1} . It was suggested that type B serrations occurred at a lower strain rate. Summarily, in DSA regime, type A serrations often occurred at low temperature, type B serrations developed with type A serrations as strain increasing, and type B serrations generally occurred at higher temperature and lower strain rate. Type C serrations often took place at a relatively high temperature compared with the temperature for the occurrence of type A and B serrations. Serrated flow always appears after critical plastic strain (ϵ_c) for the onset of the first serration, which is

vital parameter being dependent on both strain rate and temperature. Figure 5 (a) illustrates the change of critical strains for serration occurrence with different temperatures at a strain rate of $2 \times 10^{-4} \text{ s}^{-1}$. The value of ε_c decreases as temperature increasing at 450-625 °C, which verifies the occurrence of normal PLC effect. However, the value of ε_c increases with increasing temperature at 625-650 °C, indicating the occurrence of inverse PLC effect. Analogous result by Shankar [7], an inverse PLC was noticed in the temperature ($T > 550 \text{ °C}$) at $3 \times 10^{-3} \text{ s}^{-1}$, $3 \times 10^{-4} \text{ s}^{-1}$ and $3 \times 10^{-5} \text{ s}^{-1}$, where type C serrations occurred. Figure 5 (b) displays a change of critical strain for serrations with strain rates at 600 °C, it is shown that the value of ε_c increases when strain rate increased from 10^{-4} to 10^{-2} s^{-1} .

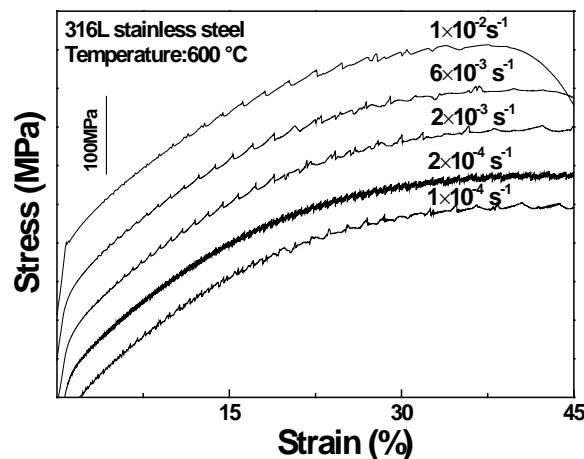


Figure 4. Segment of tensile curves at various Strain rates at 600 °C

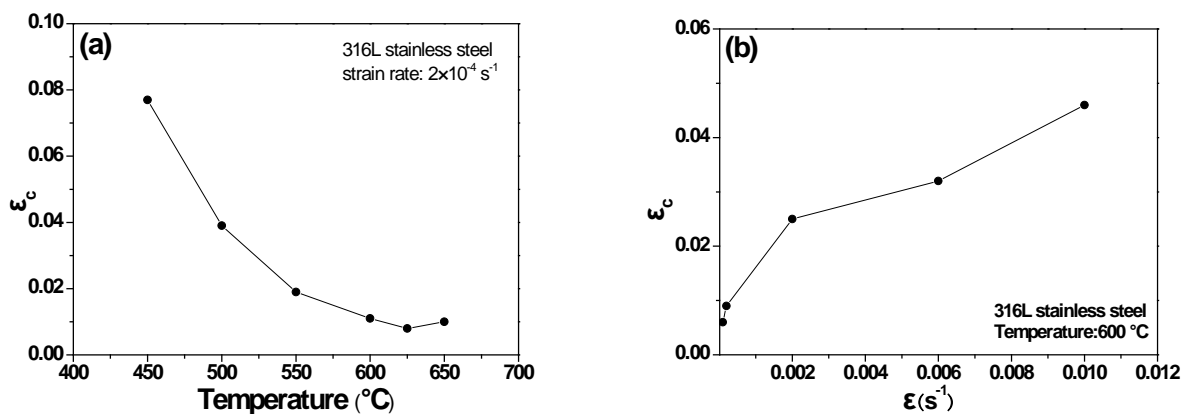


Figure 5. Plot of critical strains vs (a) temperatures at an initial strain rate of $2 \times 10^{-4} \text{ s}^{-1}$ and vs (b) strain rates at 600 °C

Due to strain can provide vacancy that contributes to the diffusion of solute atoms, a critical plastic strain is indispensable for the occurrence of DSA, which is known as vacancy-assisted solute diffusion. Diffusion velocity of solute atoms is affected significantly by temperature and strain rate. It is difficult to diffuse for solute atoms when temperature is low, then a greater strain is need at low temperature. For inverse PLC effect, some researcher guessed that solute atoms decrease at high temperature because of precipitation so that only a great strain can produce solute atoms atmosphere to pin dislocations. Likewise, the number of vacancy is small at high strain rate, therefore, there is no enough time for solute atoms to diffuse. So a greater critical plastic strain is necessary. Various models have been put forward to calculate activation energy of serrated flow causing by solute diffusion. Among these models, McCormick model is widely accepted, so activation energy associated with the

serrations can be calculated by acknowledged McCormick model [8] described by the following equation

$$\varepsilon_c^{m+\beta} = K \dot{\varepsilon} T \exp[Q_m / (RT)] \quad (1)$$

where $\dot{\varepsilon}$ is strain rate, K is Boltzmann constant, R is ideal gas constant, T is the temperature, Q_m is the activation energy for solute migration. Taking the logarithm on both sides of the Eq. (1), we can obtain the relationship as follows

$$(m + \beta) \ln \varepsilon_c = \ln K + \ln \dot{\varepsilon} + \ln T + Q_m / (RT) \quad (2)$$

If temperature is constant, the relationship can be described as

$$\ln \dot{\varepsilon} = (m + \beta) \ln \varepsilon_c + c \quad (3)$$

So the plot of $\ln \dot{\varepsilon}$ vs. $\ln \varepsilon_c$ is linear with a slope corresponding to the value of Q_m and $(m + \beta)$. The average $(m + \beta)$ value was primarily computed to be 2.17 from critical plastic strains at various strain rates at 600 °C, as showed in figure 6. The $(m + \beta)$ value for the AISI 316L stainless steel falls into the range between 2 and 3, indicating a substitution diffusion controlled mechanism of DSA.

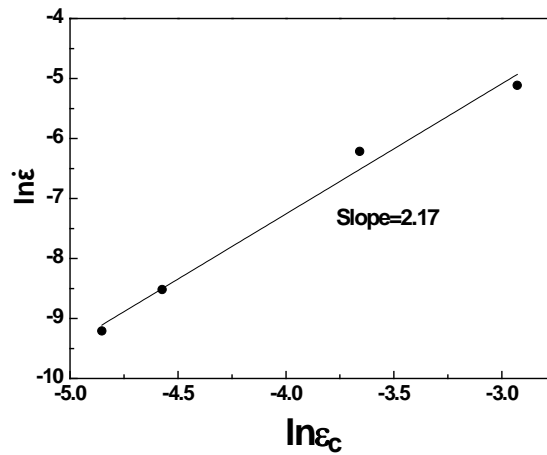


Figure 6. Relationship between critical and strain rate at 600°C

Analogously, critical plastic strain at 450, 500, 550, 600 and 625 °C is respectively 0.213, 0.082, 0.022, 0.012 and 0.009, when $\dot{\varepsilon}$ is constant. Then we can obtain the relationship as following

$$\ln(\varepsilon_c^{m+\beta} / T) = Q_m / RT + c \quad (4)$$

Hence, Q_m can be calculated according the value of $(m + \beta)$, an activation energy of 254.72 kJ/mol was obtained for types A and A+B serrations based on Eq. (4), as shown in figure 7, in agreement with previous studies. Kim et al. [5] and Samuel et al. [6] obtained an activation energy of 272 and 277-278 kJ/mol for AISI 316L stainless steel, respectively. Samuel [9] summarized activation energy data for serrated yielding in austenitic alloys, and different mechanisms were suggested. The diffusion of interstitial solute atoms (C, N and Cr for 316L) was responsible for the occurrence of DSA. Peng *et al.* [10] suggested that the mechanism of DSA in 18-8 austenitic stainless steel was attributed to solution atoms (C, Ni) atmosphere pinning the moving dislocation at a relatively low temperature range. The activation energy of these atoms for diffusion in γ -Fe is $Q_C \approx 131.2$ kJ/mol, $Q_{Mn} \approx 275.9$ kJ/mol, $Q_{Ni} \approx 282.2$ kJ/mol, $Q_{Mo} \approx 269.3$ kJ/mol and $Q_{Cr} \approx 334.4$ kJ/mol [11]. The diffusion of solute atoms in dislocation pipes need an activation energy ranging between 0.4 and 0.7 times the activation energy for bulk diffusion.

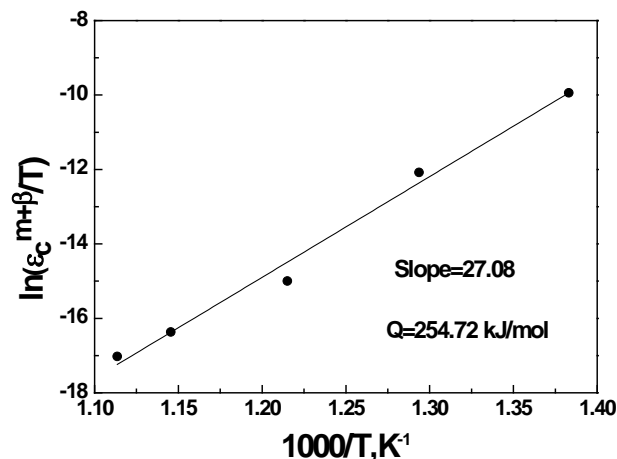


Figure 7. Variation of $\ln(\varepsilon_c^{m+\beta}/T)$ with $1000/T$ at an initial strain rate of $2 \times 10^{-4} \text{ s}^{-1}$

Considering the value of $(m+\beta)$, we considered that the mechanism of serrated flow occurred at 450-625 °C in the present 316L steel is DSA arising from the interactions between diffusing solute Cr atoms (and/or some other substitution Mn, Mo, and Ni atoms) and mobile dislocations. The species of diffusing substitution atoms giving rise to the serrated flows requires further investigation to understand detailed mechanism of serrated flow in the steel.

4. Conclusions

The serrated flow behaviour of AISI 316L austenitic stainless steel has been investigated through tensile tests at various temperatures and strain rates in combination with the calculation of activation energy for the occurrence of serrated flow. AISI 316L austenitic steel exhibits serrated flow during tensile deformation at intermediate temperatures ranging from 450 to 650 °C at an initial strain rate of $2 \times 10^{-4} \text{ s}^{-1}$. Normal PLC effect is observed at 450-625 °C, while inverse PLC effect occurs at 625-650 °C. In DSA regime, type A serrations often occur at low temperature, type B serrations develop with type A serrations as strain increasing, and type B serrations generally occur at a relatively high temperature and low strain rate. Type C serrations often take place at a higher temperature. DSA in AISI 316L austenitic stainless steel does not accompany with a plateau of yield stress, DSA leads to an increase in strength and a decrease in plasticity. Activation energy for the occurrence of serrated flows at 450-650 °C is obtained to be about 254.72 kJ/mol, suggesting that serrated flows are attributed to DSA caused by interactions between substitution Cr atoms (and or some other substitution Mn, Mo and Ni atoms) and mobile dislocations.

5. Acknowledgments

This investigation was supported by the Key Program of National Natural Science Foundation of China (Joint Funds of the National Natural Science Foundation of China and Shanghai Baosteel Group Company) (51034011), National Science and Technology Major Project (2011ZX06004-009), and ITER-National Magnetic Confinement Fusion Program (2011GB113001).

6. References

- [1] Hong S.G. and Lee S.B. 2004 *J. Nucl. Mater.* **328** 232
- [2] Choudhary B.K. 2014 *Metall. Mater. Trans. A* **45** 302
- [3] Dehghani K. and Jones J.J. 2000 *Metall. Mater. Trans. A* **31A** 1375
- [4] Tsuchida Y., Okamoto K. and Tokunaga Y. 1996 *Weld Int.* **10** 27
- [5] Kim D.W., Ryu W.S., Hong J.H. and Choi S.K. 1998 *J Mater. Sci.* **33** 675
- [6] Samuel K.G., Mannan S.L. and Rodriguez P. 1988 *Acta Metall.* **36** 2323
- [7] Shankar V., Valsan M., Rao K.B.S. and Mannan S.L. 2004 *Metall. Mater. Trans. A* **35** 3129
- [8] McCormick P.G. 1973 *Acta Metall.* **21** 873

- [9] Samuel K.G., Ray S.K. and Sasikala G. 2006 *J. Nucl. Mater.* **355** 30
- [10] Peng K.P., Qian K.W. and Chen W.Z. 2004 *Mater. Sci. Eng. A* **379** 372
- [11] Balluffi R.W. 1970 *Phys. Status Solidi B* **42** 11